# Spectrally resolved high-NA back focal plane imaging of fluorescence and nanolaser emission

F. Koenderink, H. Schokker, M. Kamp
FOM Institute AMOLF, Science Park 104 , 1098XG Amsterdam, The Netherlands (September 2013)

## Application Note

### Introduction

In nanophotonics, significant effort is devoted to creating LED's, lasers, and even single photon sources based on single quantum dots and single molecules, that have significantly improved directionality and brightness over conventional light sources [1]. The strategy of choice is to use metallic or dielectric nano-structuring in close proximity to the source material that act as so-called "plasmonic antennas" in the near field of the emitter, thereby controlling the process of emitting light directly at the source. This approach avoids the use of bulky, and potentially lossy, secondary optics that redirects light by refraction and reflection only well after it has been emitted. In order to perform quantitative experiments on such nano-antennas, a sophisticated combination of microscopy and spectroscopy is required. The first requirement is that the microscope must allow spectrally resolved fluorescence imaging with at least diffraction-limited spatial resolution to obtain spatial information on device performance, with ideally single molecule sensitivity. The second requirement is that the microscope allows back focal plane (i.e., angle-resolved) fluorescence imaging using a Bertrand lens. In this application note we discuss a third mode of operation, i.e., spectrally resolved back focal plane imaging. We apply this technique to a study of lasing in 2D distributed feedback (DFB) lasing structures that consist of a 2D periodic lattice of nano-particles embedded in a thin polymer layer that acts both as gain medium and as a planar waveguide. In our research we compare dielectric DFB lasers and "plasmonic antenna DFB lasers". In this application note we demonstrate the required instrumentation performance with data from the dielectric DFB laser systems. We show that it is possible to collect single-shot and multi-shot energy-wave vector maps of emission below and above threshold upon pumping by a ns laser pulse.

### Experiment

We use a homebuilt inverted microscope (Figure 1) in which the sample is pumped by a 532 nm microchip laser (TEEM Photonics STG-03E, <0.5 ns pulses of 3.5 μJ upon a hardware input trigger signal, at maximum 2 kHz repetition rate). The beam is either sent into the microscope as a collimated beam expanded to the back-aperture diameter to achieve maximum spatial resolution, or focused in the back-aperture plane to achieve near-collimated "epi-illumination" of a ~100 micron field of view of the sample plane.

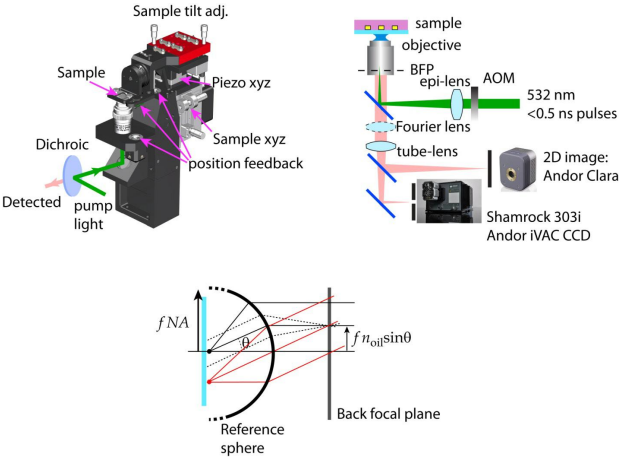


Figure 1. Left: construction diagram of our home-built inverted sample scanning fluorescence confocal microscope tower. Middle: we excite the sample using a pulsed 532 nm laser that is focused into the back-focal plane of the oil-immersion microscope objective using an "epi-lens". Power is controlled with the AOM. The excitation light forms a collimated pump beam of 100 μm across on the sample. Emission collected by the objective is used to form a real space image on the Clara CCD using just one 200 mm tube lens. Alternatively, an extra lens is flipped in to provide a back focal plane image. By flipping a flip-mounted mirror immediately after the tube lens, the real space or Fourier image is relayed to the entrance slit of a Shamrock 303i spectrograph with iVac CCD. Two relay lenses to demagnify the image to fit on the iVac CCD height (3.2 mm, smaller than the back focal plane diameter) are not shown. Right panel: the optical construction for back focal plane imaging relies on the fact that a high NA objective lens can be modeled not as an infinitely thin plane but as a "reference sphere" of radius *fNA* at which rays refracts.

Our microscope is an in-house design tower that has a fixed mount for microscope objective and 45 degree mirror, and a sample mount that can be scanned by hand (Newport Ultralign 561) and piezo-actuators (PiezoJena Tritor 100) along three axes. The design of the tower is optimized for maximum accessibility of components, and stability. The integration of 980 nm diode lasers (on the objective mount) and quadrant photocells (on the sample mount) allow calibrated distance scanning and on-line compensation of any drift and hysteresis along all three axes. Fluorescence collected by the same objective (Nikon CFI Plan APO Lambda 100x, NA = 1.45 oil) is separated from the pump light by a dichroic mirror and further cleaned by a longpass filter before detection. In the detection path, one finds a 200 mm achromatic tube lens immediately after the filters, followed by a flippable mirror that directs light either to an Andor Clara DR328G-C02-SIL CCD camera or to the entrance slit of a Shamrock SR-303i-B-SIL imaging spectrograph that uses an iVac DR324B-FI CCD detector. Since the Nikon objective is

# Spectrally resolved high-NA back focal plane imaging of fluorescence and nanolaser emission

F. Koenderink, H. Schokker, M. Kamp
FOM Institute AMOLF, Science Park 104 , 1098XG Amsterdam, The Netherlands (September 2013)

## Application Note

designed for infinity corrected use, the lens to detector distance is equal to the tube lens focal length. In this mode, i.e., with just a single tube lens, the signal at the detector corresponds to a real space image. In this way, we can perform standard spectrally integrated fluorescence imaging using the epi-illumination as pump and the Clara CCD as detector, and confocal spectral imaging by pumping just a single spot and collecting with the spectrometer. We control both the imaging read out and the spectrometric measurements using in-house developed software based on the Andor SDK to realize a synchronized measurement scheme where a National Instruments card controls sample movement (piezostage), laser timing via the laser trigger input and laser power using analog control of a acousto-optic modulator (AOM). The software allows many detection schemes, for instance integrating over exactly N laser shots (N any integer) per CCD integration frame, or conversely interspersing frames without any laser shot being fired into the measurement sequence in order to acquire background correction data.

By placing a single extra lens in between objective and tube lens, the real space imaging is converted in a Fourier space or "Back focal plane imaging" system. The basic idea is that according to the Abbe sine condition, all rays that travel from sample to objective at an angle $\theta$ from the optical axis will be focused in the back aperture at a spot at distance $f\, n \sin\theta$ from the optical axis. Here f is the focal distance of the objective (for our 100x Nikon objective $f$ = 2 mm, since the Nikon CFI60 system assumes a tube lens of 200 mm focal distance), and $n$ =1.52 is the index of the immersion medium for the objective. The optical construction for back focal plane imaging is shown in Figure 1 and relies on the fact that a high NA objective lens can be modeled not as an infinitely thin plane but as a "reference sphere" of radius $fNA$ at which rays refract. For an infinity-corrected objective, an object (black dot in Figure 1) on the optical axis will yield a collimated output beam. An object (red dot) shifted from the optical axis also yields a collimated beam but emerging at an angle from the optical axis. Rays that exit the sample from any arbitrary point in the object plane at the same angle $\theta$ will all converge to a single point in the back focal plane (BFP) at distance $f\, n \sin\theta$ from the optical axis. In actual objectives, the back focal plane is located typically just a few mm into the threaded objective back side, right at or just inside the black baffles.

A unique advantage of back focal plane imaging over, e.g., the use of a detector on a rotation stage is that a high NA objective allows to capture almost a full hemisphere of radiation pattern in a single shot measurement, with high angular resolution even when measuring on a small object. In the field of single molecule microscopy, this technique was first employed by Lieb et al. [2] to image the radiation pattern of single organic fluorophores and subsequently adopted by several workers [3-5]. According to the "reference sphere" construction in Figure 1, imaging the back focal plane intensity distribution I(x,y) on a detector array is tantamount to measuring the angle resolved flux $P(\theta,\phi)$ leaving the sample, where the 2D spatial positions (x,y) on the camera surface relate to angle as $(x,y)=nf\sin\theta$ $(\cos\phi, \sin\phi)$. Conversion to pixel number now follows simply by dividing out the pixel pitch (6.45 µm for the Clara camera). Evidently, the total back aperture diameter of a microscope objective (diameter $2f\,NA$, approximately 5 mm, is well matched to the typical size of a CCD detector). We use a factor two demagnification in order to fit the back aperture image across the spectrometer-coupled iVac CCD chip height (3.2 mm). In our setup, we either collect the full 2D back aperture without any spectral filtering on the Clara CCD detector or collect just a single slice of the 2D back aperture and disperse it into its spectral components on the spectrograph [5]. In the latter configuration, we ensure that the back focal plane image is well centered on the spectrometer slit, thereby selecting only a slice $P(\theta,\phi=0$ and $\pi)$. Dispersion by the grating ensures that the 2D image, that is projected on the iVac CCD behind the Shamrock 303i spectrograph, is a direct measure of $P(\theta,\phi=0,\pi;\lambda)$, which in solid state physics terms corresponds to a "parallel wave vector – energy" dispersion diagram.

### Choice of Detectors and Spectrograph

The choice of detectors is entirely set by signal strength considerations. We would like to be able to use our set up for sensitivity levels down to single emitters (possible upon exchange of our pump source for a cw laser or MHz repetition rate ps pulsed laser diode). As a consequence, one should be able to record a meaningful Fourier image with a photon budget of just $10^6$ photons, on par with the seminal paper by Lieb et al. [2]. If one defines "meaningful" as on the order of 100x100 pixels at least, this implies that one requires a high-quantum efficiency camera with very low readout noise with the possibility of employing hardware

# Spectrally resolved high-NA back focal plane imaging of fluorescence and nanolaser emission

F. Koenderink, H. Schokker, M. Kamp
FOM Institute AMOLF, Science Park 104 , 1098XG Amsterdam, The Netherlands (September 2013)

## Application Note

binning to further reduce readout noise and improve signal-to-noise -ratio (SNR). Given the gain material time constants of a few nanoseconds in our envisioned nanophotonic laser experiments, the imaging detectors should furthermore be suited for stroboscopic imaging: all pixels should be simultaneously charge integrating to record the nanosecond length flash of sample fluorescence that occurs during a camera exposure time of a few milliseconds. These constraints clearly favor sensitive CCD imaging devices.

Consequently we have chosen for the Andor Clara CCD camera which couples the work-horse single-molecule microscopy Sony ICX285 CCD chip with excellent read out electronics that can be set either for high frame rate (20 MHz read out clock) or lowest noise (below 2 e- readout noise for our camera at 1 MHz read out clock). We employ our camera in the lowest read-out noise setting and adjust the repetition rate of our experiment to match the required exposure time. In our work collection times per frame are so short that dark noise considerations are irrelevant.

On the spectroscopy side, we have chosen the Andor iVac CCD detector with a front illumination deep depletion CCD sensor that provides 1650 x 200 pixels that each are 16 x 16 µm in size, a peak quantum efficiency of around 60%, remaining above 20% from 425 to 975 nm, and a low read noise specified below 5.8 e-. Using 200 pixels across the height of the chip, we obtain very good effective angular resolution for our back focal plane images, corresponding to about 1 degree for a single shot spectroscopically resolved NA = 1.45 slice. By choosing either a 300 or 1200 l/mm grating, we can balance spectral resolution against SNR. In our work on nanophotonic DFB lasers, we record sequences of single shot images at increasing optical pump fluence, as controlled using a acousto-optic modulator in the laser illumination path. In this measurement scheme and especially given that we cross a lasing threshold for our samples, the main measurement limitation is dynamic range. Owing to the fact that we take essentially single shot images from a stroboscopic experiment, adjusting exposure time is not a suited method to match the detector dynamic range to the sample intensity during the measurement protocol. Since in this work for the higher sample pump powers we have an abundance of fluorescent light, we can employ a software-controlled motorized ND filter wheel in front of the detector.

### Typical Results

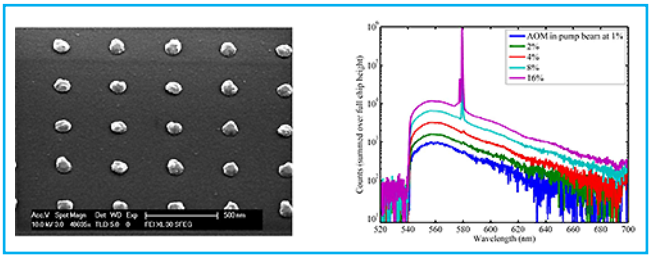


Figure 2. (a) Sample SEM image for a lattice of $TiO_2$ scatterers on glass, prior to depositing the gain-doped waveguide layer. The $TiO_2$ particles are around 90 to 100 nm across and we work with lattice spacings in the regime from 350 to 450 nm. The particles are made by first performing electron beam lithography to define a ZEP polymer resist layer (around 100 to 160 nm height) with arrays of holes and subsequent physical vapor deposition of amorphous $TiO_2$ to a nominal height of 30 nm. Finally the surrounding ZEP resist layer, which is also covered by $TiO_2$, is removed in a "lift-off" process, i.e., by soaking in a bath of NMP (N-Methyl-2-pyrrolidone). (b) Sequence of spectra at increased laser pump power as controlled by an AOM in the pump beam (selected from a sequence of 200 spectra in which the AOM range is linearly swept from 0 to 50%). A 100% setting corresponds to about 1 µJ over a spot 100 µm across. The sample consists of a lattice of $TiO_2$ particles at 380 nm pitch embedded in a R6G doped SU8 layer. A clear lasing threshold is observed at around 4 to 5% of AOM power. For large pump power, a second laser peak emerges.

To demonstrate the applicability of the setup described above, here we report results on a very simple organic DFB laser geometry. We fabricated square arrays of cylindrical dielectric scatterers ($TiO_2$, chosen for its high refractive index) of just 30 nm high and 50 nm radius on a glass substrate. After fabrication we coat the sample with a 450 nm layer of SU8 photoresist doped with Rhodamine 6G dye (on the order of 1 wt%). The SU8 material is chosen for its refractive index of around 1.65, thereby forming a 2D optical waveguiding layer for TE and for TM) that facilitates the DFB lasing process. At pitches of 375 – 420 nm, the second order in-plane Bragg diffraction condition for the waveguide mode ($\lambda$=nWGd where nWG is the guided mode index) occurs at around 590 nm wavelength, well in the R6G gain spectrum. Figure 2 shows that the system shows a clearly defined threshold pump energy (at around 0.10 µJ pulse energy spread over a 100 µm diameter area, i.e., below 0.5 mW/cm$^2$) below which the typical fluorescence spectrum of R6G is observed, and above a sharp lasing peak develops in the spectrum. Figure 3 shows a back focal plane image collected using the Clara detector at pump energy just below threshold. The back focal plane image of the sample is expected to span a circular disk, the outer diameter corresponds to exit angles $\theta$ at the objective NA ( n sin $\theta$ = NA). Converted to parallel wave vector,

# Spectrally resolved high-NA back focal plane imaging of fluorescence and nanolaser emission

F. Koenderink, H. Schokker, M. Kamp
FOM Institute AMOLF, Science Park 104 , 1098XG Amsterdam, The Netherlands (September 2013)

## Application Note

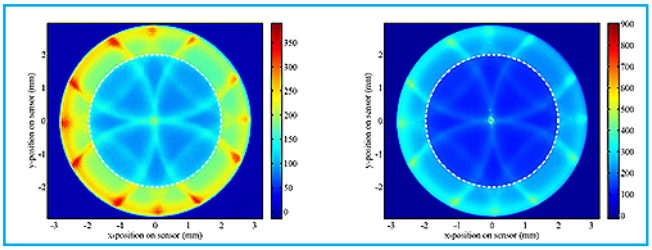

Figure 3. (a) Back focal plane image just below lasing threshold obtained on the Clara CCD camera in a single shot measurement. (b) Same just above lasing threshold. The dashed white circles correspond to NA=1, i.e. to 2 mm radius on the one-on-one image of the back focal plane on the CCD detector array. The apparent unsharpness of the diffracted circles crossing the image is due to the fact that no spectral filtering is used while the circles disperse with wavelength. This data is from the same sample as Figure 2 and 4.

the center of the image corresponds to k||=0, while the outer radius corresponds to k||=1.45 ω/c. The data shows that within this disk the outer ring, starting at an NA = 1 (white dashed line, plotted with no adjustable parameter), contains most of the emission. This observation is consistent with the well-known fact that if one places a single dipole emitter, such as a molecule or quantum dot close to an air-glass interface, most of the emission will radiate into the high-refractive index medium at angles just above the critical angle for total internal reflection. This critical angle is exactly defined as n sin θ = 1, i.e., as occurring at an NA = 1. In absence of the periodic corrugation with nanoparticles, this angular pattern is exactly known from theory and can be used to calibrate the objective NA and angle-dependent transmission function [3, 4]. In presence of the periodic grating, the back focal plane image is punctuated by curves of higher intensity. These curves in fact take the form of circles of radius nWG ω/c, concentric with the reciprocal lattice points $(k_x,k_y)=2\pi/d\ (m,n)$, and thus immediately illustrate the optical waveguide analogon of Harrisons construction of the "repeated zone scheme folded free electron dispersion" [6]. In fact, at the crossing points small stop gaps appear, pointing at multiple scattering by the periodic potential of the titania particles. The lasing above threshold occurs exactly at the crossing points. It should be noted that the folded waveguide dispersion relation in the Clara images appears unsharp because we use no spectral filter and integrate over the full dye emission spectrum.

To visualize the wavelength dispersion of the distinct bands evident on the Clara camera, we employ the Shamrock 303i spectrograph and iVac CCD detector. Figure 4 shows a raw spectrally resolved Fourier

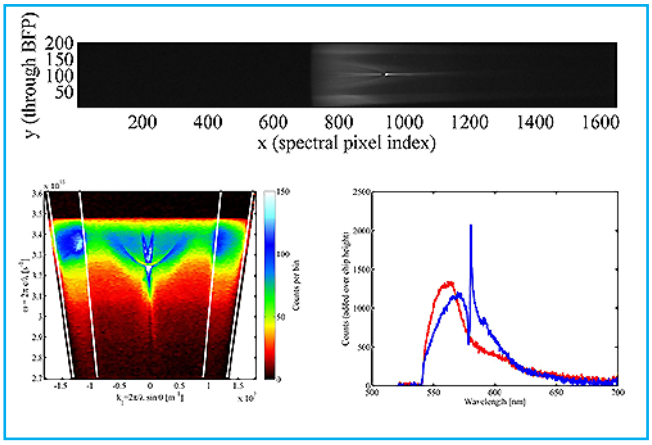


Figure 4. (a) Raw spectrally resolved back focal plane image just above lasing threshold for case as in Fig. 3(a). The pump power is at around 5% for the AOM setting (see Figure 2). (b) Same plotted as a dispersion diagram. (c) Spectra for two slices, summing over just 10 pixels vertically (software binning). The slice in blue is the central slice including the laser peak. The slice in red is taken from pixels 15 to 25, i.e. between the NA=1.45 and NA=1.0 line (white lines in (b)).

image, as well as processed data, both taken just at the lasing threshold. Again it is evident that most light escapes the sample at angles above an NA = 1. The sharp features that are evident as circles in the spectrally integrated 2D Fourier image, in the spectral $(\omega,k_x)$ diagram are seen to disperse. The features coming from the (1,0) and (-1,0) diffracted orders show a linear dispersion, the slope of which immediately yields the guided mode refractive index. Approximately at the location where they cross, a third, parabolic band appears in the diagram that corresponds to the (0, ±1) diffracted order. At the avoided crossing a lasing peak emerges, figure 4c shows spectra for two distinct slices on the iVac CCD image, i.e., for different k|| internals in the BFP image. The blue curve shows a central slice (10 pixels around θ = 0), where the laser peak is just emerging. The red curve shows the spectrum for a k|| slice far off normal, between NA = 1 and 1.45.

### Conclusion

We have realized an inverted fluorescence microscope that can be used for wide-field as well as confocal imaging. We use the microscope in particular for studies of 2D distributed feedback lasing in nanophotonic lattices of scatterers embedded in a dye-doped polymer film. The unique set up capability is to measure single shot fluorescence back focal plane images upon sub-nanosecond pulsed excitation, thereby allowing to visualize the photonic band structure that is responsible for the feedback that is required for lasing action. In

# Spectrally resolved high-NA back focal plane imaging of fluorescence and nanolaser emission

F. Koenderink, H. Schokker, M. Kamp
FOM Institute AMOLF, Science Park 104 , 1098XG Amsterdam, The Netherlands (September 2013)

## Application Note

particular, using a Clara CCD camera we can measure wavelength-integrated 2D back focal plane images, while projection of the back focal plane on the entrance slit of a Shamrock 303i spectrograph allows to spectrally disperse a single slice of wave vector space onto an iVac CCD detector. This methodology will have large use not only for studies of lasing where single-shot measurements are imperative, but also for characterizing, e.g., single molecule emission, plasmonic nanostructures, and LED performance. For the latter application, for instance, our technique can replace the mapping of emission flux as a function of angle using a photodetector on a rotation stage, a procedure that is prone to alignment errors and slow due to its sequential nature. In contrast, we record an energy-wave vector dispersion diagram in a single shot with excellent spectral resolution and with excellent angular (i.e., wave vector) resolution across almost an entire hemisphere.

**Acknowledgement**
We are grateful to Henk-Jan Boluijt for mechanical design of the inverted microscope tower (Figure 1a) and to Marco Seynen for software development on basis of the Andor SDK. This work is part of the research program of the "Stichting voor Fundamenteel Onderzoek der Materie (FOM)", which is financially supported by the "Nederlandse Organisatie voor Wetenschappelijk Onderzoek (NWO)".

**References**

[1] G. Lozano, D. J. Louwers, S. R. K. Rodriguez, S. Murai, O. T. A. Jansen, M. A. Verschuuren, J. G. Rivas, Plasmonics for solid-state lighting: enhanced excitation and directional emission of highly efficient light sources, NPG: Light: Science & Applications 2, e66 (2012).
[2] M. A. Lieb, J. M. Zavislan, and L. Novotny, Single-molecule orientations determined by direct emission pattern imaging, J. Opt. Soc. Am. B 21, 1210 (2004).
[3] T. H. Taminiau, S. Karaveli, N. F. van Hulst, and R. Zia, Quantifying the magnetic nature of light emission, Nature Comm. 3, 979 (2012).
[4] L. Dai, I. Grego, I. von der Hocht, T. Ruckstuhl, J. Enderlein, Measuring large numerical apertures by imaging the angular distribution of radiation of fluorescing molecules, Opt. Express 13, 9409 (2005).
[5]. I. Sersic, C. Tuambilangana and A. F. Koenderink, Fourier microscopy of single plasmonic scatterers, New. J. Phys 13 083019:1-14, (2011).
[6] N.W. Ashcroft and N. D. Mermin, Solid State Physics, Intn'l edition, Saunders College Publishing (1976). Consult Chapter 9, page 172-173, exercise 5.

**Contact**

Prof. Dr. A. F. Koenderink
Center for Nanophotonics
FOM Institute AMOLF
Science Park 104
1098 XG Amsterdam
The Netherlands

Phone: +31-20-754 7189
E-mail: fkoenderink@amolf.nl
Web: www.amolf.nl